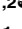





## RESEARCH ARTICLE

## Lipidomics of human adipose tissue reveals diversity between body areas

Naba Al-Sari<sup>1,2</sup>, Tommi Suvitaival<sup>1</sup>\*, Ismo Mattila<sup>1</sup>, Ashfaq Ali<sup>1</sup><sup>aa</sup>, Linda Ahonen<sup>1</sup><sup>ab</sup>, Kajetan Trost<sup>1</sup>, Trine Foged Henriksen<sup>3</sup>, Flemming Pociot<sup>1,2</sup>, Lars Ove Dragsted<sup>4</sup>, Cristina Legido-Quigley<sup>1,5</sup>

**1** Steno Diabetes Center Copenhagen, Gentofte, Denmark, **2** Dept. of Clinical Medicine, University of Copenhagen, Gentofte, Denmark, **3** Capio CFR, Kgs. Lyngby, Denmark, **4** Dept. Nutrition, Exercise and Sports, University of Copenhagen, Gentofte, Denmark, **5** Institute of Pharmaceutical Science, King's College London, London, United Kingdom

 These authors contributed equally to this work.

<sup>aa</sup> Current address: National Bioinformatics Infrastructure Sweden, Uppsala, Sweden

<sup>ab</sup> Current address: Biosyntia ApS, Copenhagen, Denmark

\* [tommi.raimo.leo.suvitaival@regionh.dk](mailto:tommi.raimo.leo.suvitaival@regionh.dk)


 OPEN ACCESS

**Citation:** Al-Sari N, Suvitaival T, Mattila I, Ali A, Ahonen L, Trost K, et al. (2020) Lipidomics of human adipose tissue reveals diversity between body areas. PLoS ONE 15(6): e0228521. <https://doi.org/10.1371/journal.pone.0228521>

**Editor:** Monika Oberer, Karl-Franzens-Universitat Graz, AUSTRIA

**Received:** January 16, 2020

**Accepted:** May 15, 2020

**Published:** June 16, 2020

**Copyright:** © 2020 Al-Sari et al. This is an open access article distributed under the terms of the [Creative Commons Attribution License](https://creativecommons.org/licenses/by/4.0/), which permits unrestricted use, distribution, and reproduction in any medium, provided the original author and source are credited.

**Data Availability Statement:** All relevant data are within the manuscript and its Supporting Information files.

**Funding:** The authors received no specific funding for this work. The work was carried out at and paid by Steno Diabetes Center Copenhagen. Capio CFR provided sample material but did not provide funding. Biosyntia ApS did not provide funding and was not involved in the study at the time of carrying out the study. Apart from Trine Foged Henriksen, all authors were employees of Steno Diabetes Center Copenhagen at the time of carrying

## Abstract

### Background and aims

Adipose tissue plays a pivotal role in storing excess fat and its composition reflects the history of person's lifestyle and metabolic health. Broad profiling of lipids with mass spectrometry has potential for uncovering new knowledge on the pathology of obesity, metabolic syndrome, diabetes and other related conditions. Here, we developed a lipidomic method for analyzing human subcutaneous adipose biopsies. We applied the method to four body areas to understand the differences in lipid composition between these areas.

### Materials and methods

Adipose tissue biopsies from 10 participants were analyzed using ultra-high-performance liquid chromatography coupled to quadrupole time-of-flight mass spectrometry. The sample preparation optimization included the optimization of the lipid extraction, the sample amount and the sample dilution factor to detect lipids in an appropriate concentration range. Lipidomic analyses were performed for adipose tissue collected from the abdomen, breast, thigh and lower back. Differences in lipid levels between tissues were visualized with heatmaps.

### Results

Lipidomic analysis on human adipose biopsies lead to the identification of 186 lipids in 2 mg of sample. Technical variation of the lipid-class specific internal standards were below 5%, thus indicating acceptable repeatability. Triacylglycerols were highly represented in the adipose tissue samples, and lipids from 13 lipid classes were identified. Long polyunsaturated triacylglycerols in higher levels in thigh ( $q < 0.05$ ), when compared with the abdomen, breast and lower back, indicating that the lipidome was area-specific.

out the study. Capio CFR and Biosyntia ApS did not have any additional role in the study design, data collection and analysis, decision to publish, or preparation of the manuscript.

**Competing interests:** Trine Foged Henriksen is an employee of Capio CFR, which is a private hospital. Linda Ahonen is currently an employee of Biosyntia ApS, which is a company operating in the field of bioprocess technology. This does not alter our adherence to PLOS ONE policies on sharing data and materials.

## Conclusion

The method presented here is suitable for the analysis of lipid profiles in 2 mg of adipose tissue. The amount of fat across the body is important for health but we argue that also the distribution and the particular profile of the lipidome may be relevant for metabolic outcomes. We suggest that the method presented in this paper could be useful for detecting such aberrations.

## 1. Introduction

Adipocytes are cells that form and store lipids in adipose tissue, they play a major role in energy homeostasis [1,2]. Obesity, which is characterized by increased storage of lipids in adipose tissue and modification of the metabolic functions of adipocytes, is a risk factor for several metabolic diseases, including atherosclerosis, cardiovascular ischemic disease, hypertension, hyperglycemia and insulin resistance in type 2 diabetes[1,3,4,5,6,7]. The molecular composition of adipose tissue may reveal its functionality and links to metabolic disease[8,2]. In addition, lipid deposition is important because individuals, who have more visceral adipose tissue, have a greater risk of metabolic disease[9]. Hence, global lipidomic analysis of multiple areas of adipose tissue may lead to a better understanding of metabolism in disease[10,11].

Lipidomics, together with genomics, transcriptomics, and proteomics, can give new biological insights and reveal novel metabolic pathways[12,13,14,15,16,17]. As an ‘-omics’ field, lipidomics is the approach of choice to understanding lipid biology[12,18,19,20]. Particularly, lipid composition of adipose tissue can reflect the long-term consumption of lipids[21]: adipose tissue has been shown to reflect dairy fat consumption at an annual level, whereas blood reflects the dietary intake over a time scale of weeks to months[22,23].

Lipidomics technologies can be used to measure hundreds of lipids in human biofluid or tissue[12,24]. However, few lipidomic analysis have been performed on human adipose tissue [25,26,27]. Lipidomics is a platform-dependent technique and numerous sample preparation methods have been reported[28,29,30,31,32]. Although there is no single technique to extract and cover the entire lipidome, the most common sample preparation techniques are variations of the liquid-liquid extraction (LLE) using the Folch extraction and the LLE using methyl *tert*-butyl ether (MTBE), originally introduced by Matyesh et al.[33,24]. Lipids from adipose tissue have also been extracted with a mixture of isooctane and ethyl acetate[29].

Here, we developed a method for a broad-coverage lipidomic analysis of human adipose biopsies that could be used at a clinical mass-spectrometry lab. The method was applied to adipose tissue samples from four body areas to identify possible compositional differences. The method resulted on annotation of nearly 200 lipids from adipose tissue in this small cohort of obese participants. We observed that thigh subcutaneous adipose tissue had a different lipid profile compared to biopsies obtained from the back, abdomen and breast, whereas the three other areas were largely similar by their lipid composition.

## 2. Materials and methods

### 2.1 Ethics statement

According to the European and national legislation ethical approvals are needed only for trials where subjects are volunteering to a treatment and/or where data are collected in a way that allows identification of the individual from whom they originate. In the current study the

samples were collected completely anonymously as waste materials from a fat suction clinic, which means there is no way by which it is possible to trace them back to any individuals. No logs were made and while the subjects gave oral consent to their fat waste being used anonymously, no records were made on who gave which samples, only on where on the body they originated. Data collected in a completely anonymous way is exempt from European and national ethics and data safety regulations. Since the GDPR regulation was new at the time we asked for (and received) approval of data transfer but in fact that was also not needed.

## 2.2 Chemicals

Methanol (MeOH) and water (H<sub>2</sub>O) of LC-MS grade was purchased from Honeywell (Morris Plains, NJ, USA). Chloroform (CHCl<sub>3</sub>), methyl-tert-butyl ether (MTBE) and Sodium chloride (NaCl) of reagent grade were purchased from Sigma-Aldrich (Steinheim, Germany).

Stock solutions (1 mg mL<sup>-1</sup>) of chosen lipid standards were prepared in CHCl<sub>3</sub>:MeOH (2:1, v/v). The following of these lipid standards were purchased from Sigma-Aldrich: 1,2-dimyristoyl-*sn*-glycero-3-phospho(choline-d13) (PC(14:0/14:0)-d13), 1,2,3-triheptadecanoylglycerol (TG(17:0/17:0/17:0)) and 3β-hydroxy-5-cholestene 3-linoleate (ChoE(18:2)). 1,2-diheptadecanoyl-*sn*-glycero-3-phosphoethanolamine (PE(17:0/17:0)), N-heptadecanoyl-D-*erythro*-sphingosylphosphorylcholine (SM(d18:1/17:0)), N-heptadecanoyl-D-*erythro*-sphingosine (Cer(d18:1/17:0)), 1,2-diheptadecanoyl-*sn*-glycero-3-phosphocholine (PC(17:0/17:0)), 1-heptadecanoyl-2-hydroxy-*sn*-glycero-3-phosphocholine (LPC(17:0)), 1-palmitoyl-d31-2-oleoyl-*sn*-glycero-3-phosphocholine (PC(16:0/18:1)-d31), 1-hexadecyl-2-(9Z-octadecenoyl)-*sn*-glycero-3-phosphocholine (PC(16:0e/18:1(9Z))), 1-(1Z-octadecenyl)-2-(9Z-octadecenoyl)-*sn*-glycero-3-phosphocholine (PC(18:0p/18:1(9Z))), 1-octadecanoyl-*sn*-glycero-3-phosphocholine (LPC(18:0)), 1-(1Z-octadecenyl)-2-docosahexaenoyl-*sn*-glycero-3-phosphocholine (PC(18:0p/22:6)). 1-stearoyl-2-linoleoyl-*sn*-glycerol (DG(18:0/20:4)) was purchased from Avanti Polar Lipids, Inc. (Alabaster, AL, USA) and tripalmitin-1,1,1-13C3 (TG(16:0/16:0/16:0)-13C3), trioctanoin-1,1,1-13C3 (TG(8:0/8:0/8:0)-13C3) and 1-palmitoyl-2-hydroxy-*sn*-Glycero-3phosphatidylcholine (LPC(16:0)) from Larodan AB (Solna, Sweden). A working standards solution (StdMix) was then prepared from these stock solutions into a concentration of 10 μg mL<sup>-1</sup> in CHCl<sub>3</sub>:MeOH (2.1, v/v).

Additionally, the following quality control samples were prepared: blanks (solvent and matrix blanks), standard mixture samples, standard reference material (NIST 1950), pooled plasma samples and pooled adipose tissue samples. The pooled plasma samples and the NIST samples were prepared according to the following procedure: 10 μl aliquoted pooled plasma samples were thawed on ice. 10 μl 0.9% NaCl, 28 μl StdMix (10 μg/ml) were then added to the samples and extracted with 92 μl of CHCl<sub>3</sub>:MeOH (2:1, v/v).

## 2.3 Sample preparation and sample analyses

Approximately 20g waste materials from the suction were randomly collected. The 17 collected samples were from different body areas, abdomen (N = 6), breast (N = 3), thigh (N = 4) and lower back (N = 4) from a total of N = 10 participants. All the collected samples were transferred to Steno Diabetes Center Copenhagen (SDCC) on dry ice and were stored at -80 °C in collection tubes until analysis and the remaining samples were then discarded.

A section of adipose tissue sample was cut from each sample with a scalpel and loaded into the center of a tissue tube using a spatula. Transfer tubes were screwed onto the tissue tubes and the tubes were treated with liquid nitrogen for approximately 1 min to flash-freeze the tissue. The flash-frozen adipose tissue was cryopulverized using a CryoPREP™CP02 Pulverizer (Covaris Inc., USA), flash-frozen again and pulverized a second time. A given amount was

weighed out from each sample and stored at  $-80^{\circ}\text{C}$  until lipid extraction and analyses. All samples were randomized before sample preparation and again before analysis. Two different lipid extraction procedures (a modified Folch extraction procedure and a procedure based on extraction with MeOH:MTBE) were applied to the pulverized adipose tissue samples in order to determine the best procedure to use for further clinical studies.

The two different lipid extraction methods were initially performed on a sample from the abdomen of one subject using four replicates of cryopulverized samples ( $10\text{ mg} \pm \text{SD}: 0.68\text{ mg}$ ) in 1 $\times$ , 5 $\times$ , 10 $\times$ , 20 $\times$ , 40 $\times$ , 80 $\times$  and 100 $\times$  dilutions. Four replicates of homogenate samples were extracted using the  $\text{CHCl}_3$ :MeOH extraction procedure and four replicates of homogenate samples from one subject were extracted using the MeOH:MTBE extraction procedure. The modified Folch extraction procedure was performed as follows: first 200  $\mu\text{L}$  of 0.9% NaCl was added to the cryopulverized adipose tissue samples. The samples were then spiked with 136  $\mu\text{L}$  of a  $10\text{ }\mu\text{g mL}^{-1}$  StdMix and extracted with 344  $\mu\text{L}$  of  $\text{CHCl}_3$ :MeOH (2:1, v/v). The samples were then vortex mixed, sonicated for 5 min, vortex mixed again and incubated on ice for 30 min. Finally, the samples were centrifuge at 10000 *rpm* for 3 min at  $4^{\circ}\text{C}$ . The lower phase (100  $\mu\text{L}$ ) was then pipetted into a new Eppendorf tube and 100  $\mu\text{L}$  of  $\text{CHCl}_3$ :MeOH (2:1, v/v) was added. The samples were further diluted in a range of dilutions (1, 5, 10, 20, 40, 80 and 100 times) for different purposes as described below. The samples were stored at  $-80^{\circ}\text{C}$  until analysis.

The extraction procedure utilizing a mixture of MeOH and MTBE was somewhat different from the modified Folch extraction procedure. Here, 188  $\mu\text{L}$  of  $\text{H}_2\text{O}$  was added to the cryopulverized adipose tissue samples and the samples were then extracted with 975  $\mu\text{L}$  of MeOH:MTBE:StdMix (225:750:35, v/v/v). The samples were vortex-mixed, sonicated for 5 min, vortex-mixed again and incubated on ice for 30 min. Finally, the samples were centrifuged at 10000 *rpm* for 3 min ( $4^{\circ}\text{C}$ ) and 350  $\mu\text{L}$  of the upper phase was pipetted into a new Eppendorf tube. The samples were then dried to completeness under nitrogen ( $\text{N}_2$ ). The samples were reconstituted in 110  $\mu\text{L}$  of  $\text{CHCl}_3$ :MeOH (2:1, v/v) and diluted serially (1, 5, 10, 20, 40, 80 and 100 times). The samples were stored at  $-80^{\circ}\text{C}$  until analysis. Once the samples had been prepared, they were analyzed using a previously published ultra-high-performance liquid chromatography quadrupole time-of-flight mass spectrometry method (UHPLC-Q-TOF-MS) [34,35,36,37]. See [S1 Method](#) for detailed description of the LC-MS method. All data were acquired using the MassHunter B.06.01 software by Agilent Technologies (Waldbronn).

## 2.4 Data processing

The acquired data were pre-processed with MZmine (version 2.28) and peaks were annotated based on an in-house peak library and the LIPID MAPS<sup>®</sup> database[38,39]. The peaks from the internal standards were detected by targeted analyses from the standard sample analyses to normalize each feature against internal standards in R. The other peaks in the samples were processed as follows: Mass detection was performed keeping the noise level at 1.5E3. Chromatogram builder used a minimum time span of 0.06 min, minimum height of 4.5E3, and *m/z* tolerance of 0.006 (or 10 ppm). Local minimum search algorithm was used for chromatogram deconvolution with a 70% chromatographic threshold, 0.05 min minimum RT range, minimum relative height 5%, minimum absolute height 7.5E3, minimum ratio of peak top/edge 1, and peak duration range 0.06–2.0 min.

Chromatograms were then deisotoped by using the isotopic peaks grouper algorithm with a *m/z* tolerance of 0.001 (or 2.0 ppm) and a RT tolerance of 0.05 min, following which the most abundant ion was kept. The peak list was filtered for exclude false signals and then row filtered for removing all rows which did not meet the requirement of minimum 1 peak in a row. Peak

alignment was achieved using the join aligner method ( $m/z$  tolerance 0.006 (or 10.0 ppm), weight 2 for  $m/z$ , absolute RT tolerance 0.2 min), absolute RT tolerance of 1 min, and a threshold value of 1. Peak list row filtered again with minimum of 15 peaks in a row. The peak list was gap-filled with the same RT and  $m/z$  range gap filler ( $m/z$  tolerance at 0.006 or 10.0 ppm). Peak list was filtered again, and row filtered. Finally, the peak list was annotated using internal library with an  $m/z$  tolerance of 0.006  $m/z$  or 10.0 ppm and a RT tolerance of 0.2 min.

The peak list was imported to R and each feature was normalized against an internal standard. The annotation included features, which had the same RT and  $m/z$  value as compounds in NIST 1950 serum samples[40]. Features that corresponded to equivalent standards injected during the sequence were labeled as Level 1 and features with structure information were labeled as Level 2[41]. Coefficient of variation (or, relative standard deviation; %RSD) for peak areas and retention times of lipid-class specific internal standards were calculated.

## 2.5 Statistical analysis

Statistical analysis were performed with R (<http://www.r-project.org/>) [42]. The overall variation in samples were visualized in a principal component analysis (PCA) plot with annotation of the body area using the FactoMineR package [43]. Lipid-specific variation between body areas was assessed with lipid-wise linear regression models using the limma package, and the resulting model coefficients and their statistical significance were visualized on heatmaps using the ggplot2 package [44,45]. Lipid species with the biggest change were visualized in box-plots grouped by body area. Results of the statistical tests were corrected for multiple testing using the Benjamini-Hochberg method.

## 3. Results and discussion

### 3.1 Method development

There are several protocols for lipidomics analyses suitable for the isolation and purification of lipids from blood and tissue samples [24,34,46,47,48]. The most widely used are based on the Folch extraction and an MTBE based method described by Matyash *et al.* [24,49]. To the knowledge of the authors, neither of these methods have so far been applied to human adipose tissue from different body sampling sites.

The aim of this study was to establish an optimal analytical procedure for multi-area adipose tissue lipidomics. Initially, two different extraction techniques (a modified Folch technique and an MTBE based technique) and two sample amounts and serial sample dilutions were tested. The optimization was made considering the number of annotated lipid features (unique retention time and  $m/z$  pairs) while minimizing peak saturation.

Both extraction methods—the  $\text{CHCl}_3$ :MeOH and the MeOH:MTBE—consistently gave the same features. We progressed with the modified FOLCH method, since it has been proven to be feasible for high-throughput use in lipidomics analysis. The results also suggested that 10 mg resulted in a saturation of peaks. A 20 $\times$  dilution was deemed as the best dilution when considering the lipid features and lipid class abundance. The  $\text{CHCl}_3$ :MeOH method with a sample amount of 2 mg  $\pm$  SD: 0.41 mg and a dilution factor of 20 $\times$  was hence determined as the optimal approach. In this protocol we aimed to minimize the starting material and focus on lipids that are abundant in adipose tissue, such as the triacylglycerols.

### 3.2 Overall lipid composition in adipose tissue

Adipose tissue samples from different body areas were analyzed using the optimized sample preparation method. The areas (abdomen,  $N = 6$ ; breast,  $N = 3$ ; lower back,  $N = 4$ ; and thigh,

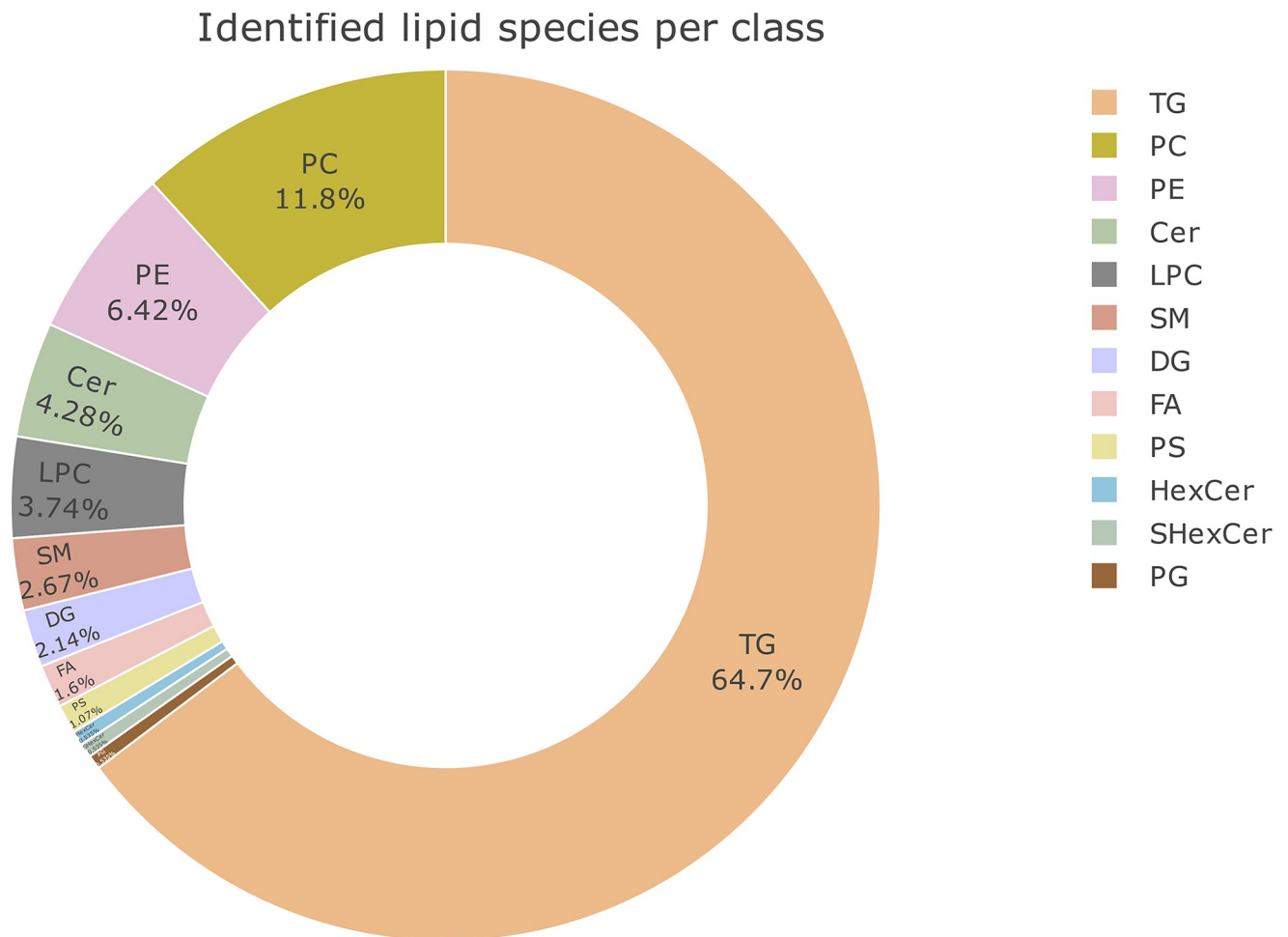


**Fig 1.** Donut plot showing numbers of lipids detected from each class and their proportion (%) among the identified lipids in adipose tissue. The result is from the optimized method.

<https://doi.org/10.1371/journal.pone.0228521.g001>

$N = 4$ ) resulted in 186 lipid features from a 2 mg sample. These lipid features belonged to 13 major classes of lipids dominated by the triacylglycerols (TGs; [S1](#) and [S2](#) Tables). Also the following lipid classes were detected: diacylglycerols (DGs), ceramides (Cers), fatty acids (FAs), hexocyl-ceramides (HxCers), lyso-phosphatidylcholines (LPCs), phosphatidylcholines (PCs), alkyl-acyl phosphatidylcholines (PC-Os or PC-Ps), phosphatidylglycerols (PGs), phosphatidylethanolamines (PEs), alkyl-acyl phosphatidylethanolamines (PE-Os or PE-Ps), phosphatidylserines (PSs) and sphingomyelins (SMs).

Data from positive ion mode, which was analyzed further, covered eight of these lipid classes (DGs, HxCers, LPCs, PCs, PC-Os or PCPs, SMs and TGs). The relative numbers of identified lipids from these classes are shown in [Fig 1](#) and all the identified lipids from positive as well as negative ion mode are listed in [S1](#) and [S2](#) Tables.

Analysis of technical variation indicated that the method was reproducible throughout the sample set. The coefficient of variation (or, relative standard deviation; RSD;%) of the peak areas were on average 4.8% and retention time were on average 0.3% for the internal standards ([Table 1](#)).

A principal component analyses (PCA) of the lipid profiles revealed a 5multivariate pattern of the overall variation in the data ([Fig 2](#)). The results show that the adipose biopsy samples

**Table 1. Technical variation in the analysis.** Shown in the table are the coefficient of variation (or, relative standard deviation; RSD;%) for peak area and retention time (RT) of the internal standards in adipose tissue samples.

Name	%RSD: peak area	%RSD: RT
01. PE(17:0/17:0)	3.71	0.08
02. SM(d18:1/17:0)	1.39	0.10
03. Cer(d18:1/17:0)	17.96	0.15
04. PC(17:0/17:0)	2.16	0.51
05. LPC(17:0)	0.98	0.82
06. PC(14:0/14:0)-d13	1.13	0.72
07. TG(16:0/16:0/16:0)-13C3	16.86	0.08
08. TG(8:0/8:0/8:0)-13C3	1.76	0.07
09. PC(16:0/18:1)-d31	0.85	0.12
09b. PC(16:0/18:1)-d30	0.78	0.10
AVERAGE	4.76	0.28

Abbreviations: PE, phosphatidylethanolamine; SM, sphingomyelin; Cer, Ceramides; PC, phosphatidylcholine; LPC, lysophosphatidylcholine and TG, triacylglycerol.

<https://doi.org/10.1371/journal.pone.0228521.t001>

from the thigh clustered in the lower half of the projection and the pooled adipose tissue samples (crosses) clustered in the middle as an indication of method reproducibility.

Next, lipid levels were individually compared between the body areas to find out, whether the body's lipid composition is location-specific. Levels of each lipid species were compared pair-wise between different areas. These comparisons are illustrated in the diagram of Fig 3A.

Thigh appeared the most distinct adipose tissue among the body areas. Thereby, we start by describing the distinct lipid profile of the adipose tissue in thigh.

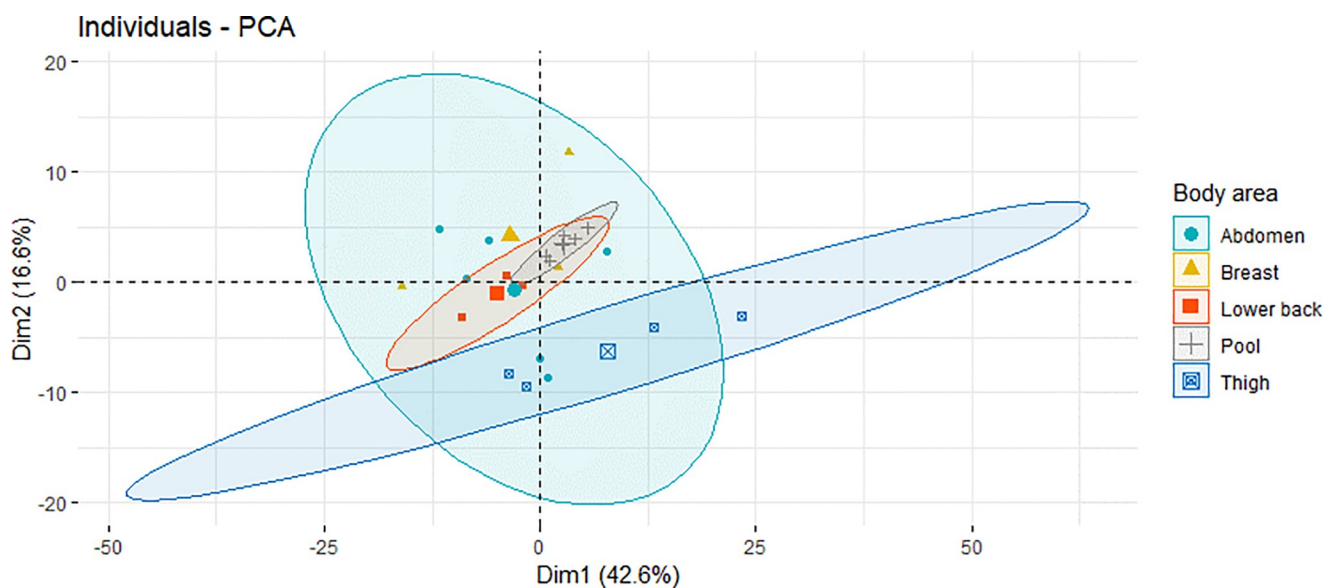


**Fig 2. Principal component analysis (PCA) plot showing individual and technical variation (pooled samples as grey crosses).** PCA summarizes the multivariate pattern of overall variation in the data that come from adipose tissue samples ( $n = 17$ ) from four body areas. The first two principal axes are shown on the x-axis and y-axis, respectively. Thigh (blue squares) is distinct from abdomen (blue circles), breast (yellow triangles) and lower back (red squares). The centroids of the sample groups are shown as larger-sized symbols and the two-standard-deviation (95%) confidence intervals of the sample groups around the centroids are shown as ellipsoids.

<https://doi.org/10.1371/journal.pone.0228521.g002>

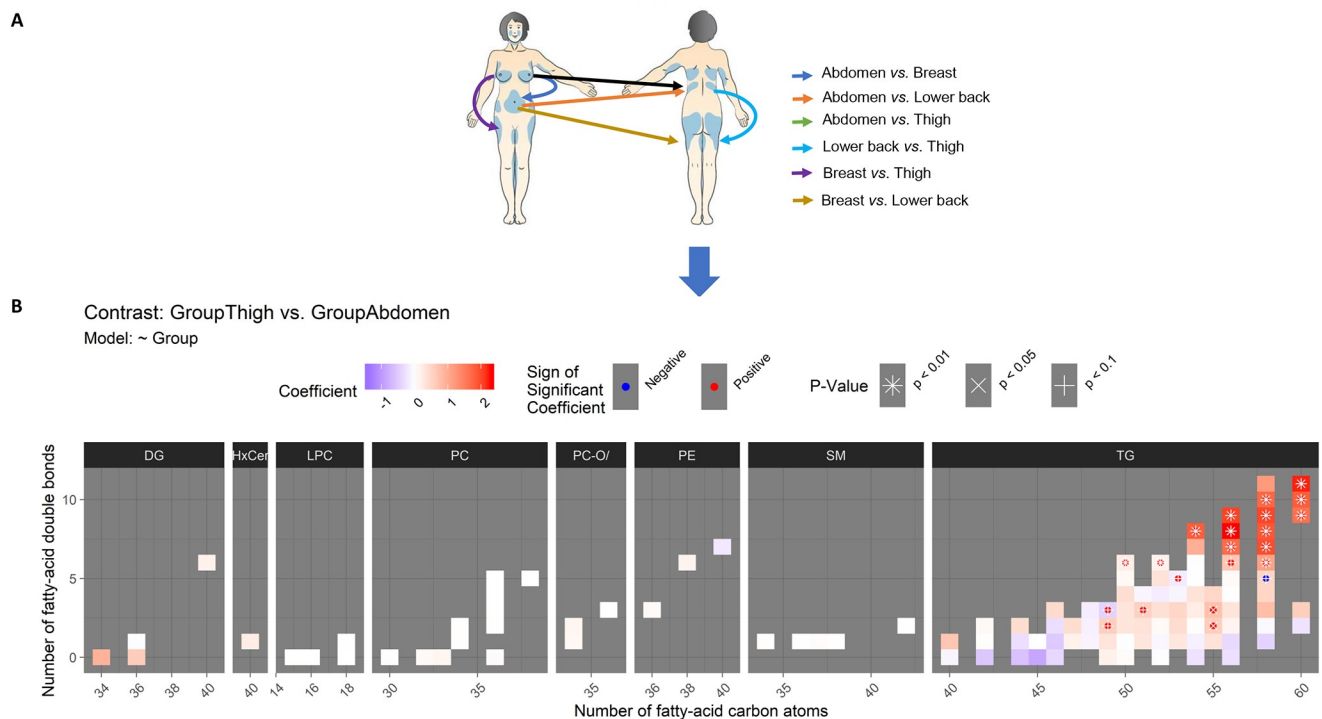


**Fig 3.** (A) Diagram illustrating all the pair-wise comparisons between adipose tissue samples from different body areas. Results of these comparisons are shown in Figs 3B and 4 and S1 Fig. (B) Difference in the lipidome between thigh and abdomen. Lipids are grouped by their class into panels (in columns from DG to TG). Within each panel, each colored rectangle corresponds to one lipid species, and its location in the x-axis and y-axis, respectively, shows its size (number of carbon atoms in the fatty acid chains) and its level of unsaturation (number of double bonds). Blue, red and white rectangles, respectively, indicate lower, higher and same levels in thigh compared to abdomen (based on the regression coefficient from the linear regression model with the body area as an independent variable and the lipid level as the dependent variable). Statistical significance of the difference is annotated by the symbols “\*”, “X” and “+,” respectively, corresponding to  $p < 0.01$ ,  $0.05$  and  $0.1$ . For instance, the triacylglycerol TG(60:11), located in the x- and y-coordinates 60 and 11, respectively, (the top-rightmost corner) in the TG panel, has a total of 60 carbon atoms and 11 double bonds (i.e., unsaturated bonds) in its fatty-acid chains. The lipid TG(60:11) has a clearly higher level in thigh compared to abdomen (red color of the rectangle) with a statistical significance of  $p < 0.01$  (annotation with the character “\*”).

<https://doi.org/10.1371/journal.pone.0228521.g003>

### 3.3 Differences between thigh and other body areas

First, thigh was compared to abdomen (Fig 3B). The levels of all long polyunsaturated triacylglycerols (TGs) with more than 55 carbon atoms and five double-bonds were higher in thigh, and in all but two of these 13 TGs, the difference was significant at  $p < 0.01$  after correction for multiple testing. This pattern can be seen in the top-right corner of the TG panel in Fig 3B with positive model coefficients (in red color) of these TG lipids. Furthermore, five mid-sized polyunsaturated TGs with 50 to 55 carbon atoms and two to six double bonds had higher levels in thigh at  $p < 0.05$  (see the red-colored middle-right part of the TG panel in Fig 3B).

Second, the difference between thigh and lower back adipose tissue was broadly similar to the difference between thigh and abdomen (Fig 4A). Also when compared to lower back, thigh had higher levels of long polyunsaturated TGs (see the top-right part of the TG panel in Fig 4A). Although three of these TGs were higher only at  $p < 0.05$ , nine other TGs were higher at  $p < 0.01$ . More mid-sized polyunsaturated TGs (with 50 to 55 carbon atoms and two to six double bonds) were different between thigh and lower back than thigh and abdomen: The levels of nine mid-sized polyunsaturated TGs (with 50 to 55 carbon atoms and two to six double bonds) were higher in thigh at  $p < 0.05$  (see the middle-right part of the TG panel in Fig 4A). This was more than the six, which were previously found different between thigh and



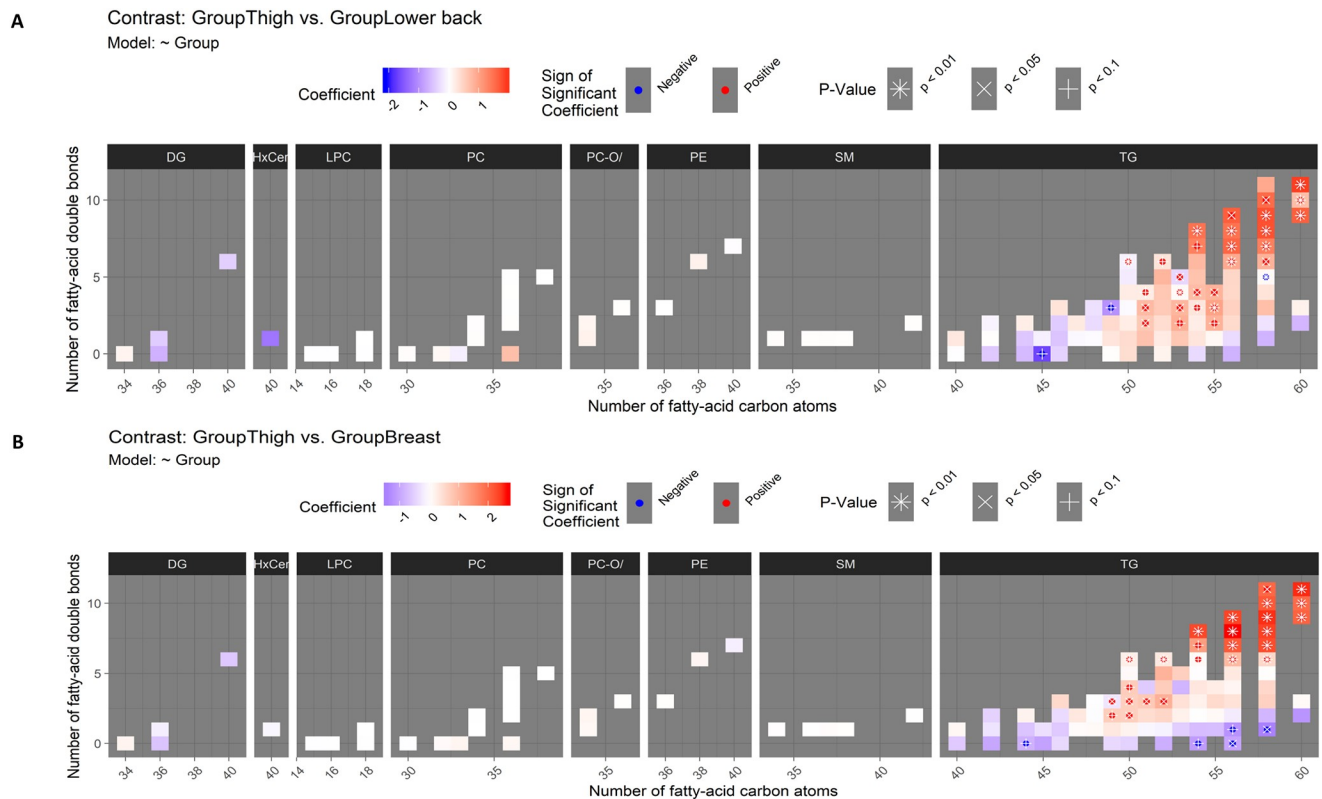


**Fig 4.** (A) Difference in the lipidome between thigh and lower back. See instructions for interpreting the figure in the caption of Fig 3B. (B) Difference in the lipidome between thigh and breast.

<https://doi.org/10.1371/journal.pone.0228521.g004>

abdomen. Unlike against abdomen, TG(58:5) was lower in thigh compared to lower back ( $p < 0.01$ ; see the TG panel of Fig 4A at x-axis value 58 and y-axis value 5).

Again, in the comparison between thigh and breast, long polyunsaturated TGs appeared with clearly higher levels in thigh (Fig 4B): all 13 of these TGs were higher at  $p < 0.05$  and only the weakest difference with TG(58:11) did not reach  $p < 0.01$ . Also a group of mid-sized TGs was again at higher levels in thigh than in breast but in this comparison the difference was confined to TGs with 49 to 52 carbon atoms instead of the up to 55 carbon atoms observed in the previous comparisons. The lower level of saturated and monounsaturated TGs in thigh compared to breast was more pronounced than in the comparisons involving thigh (see the bottom-part of the TG panel in Fig 4B): TG(56:0) and TG(58:1) were lower in thigh at  $p < 0.05$ . Boxplots of the triacylglycerols TG (60:11) and TG(58:8), which was one of the lipids with highest difference between the body areas are shown in Fig 5.

Other lipid classes did not have differences between thigh and other areas at  $p < 0.05$  although non-significant patterns in DGs, HexCers and PCs were visible in Figs 3B and 4.

### 3.4 Differences between lower back, breast and abdomen

Only minor differences were observed between lower back and breast, when putting to the perspective of the rather rich signature of differences between thigh and other body areas. At  $p < 0.05$ , lower back had higher levels of the polyunsaturated TGs 52:6, 56:7 and 58:8 (see the top-right quarter of the panel in the “Lower Back vs. Breast” column and “TG” row in the S1 Fig). In a broader pattern of non-significant differences, lower back had generally higher

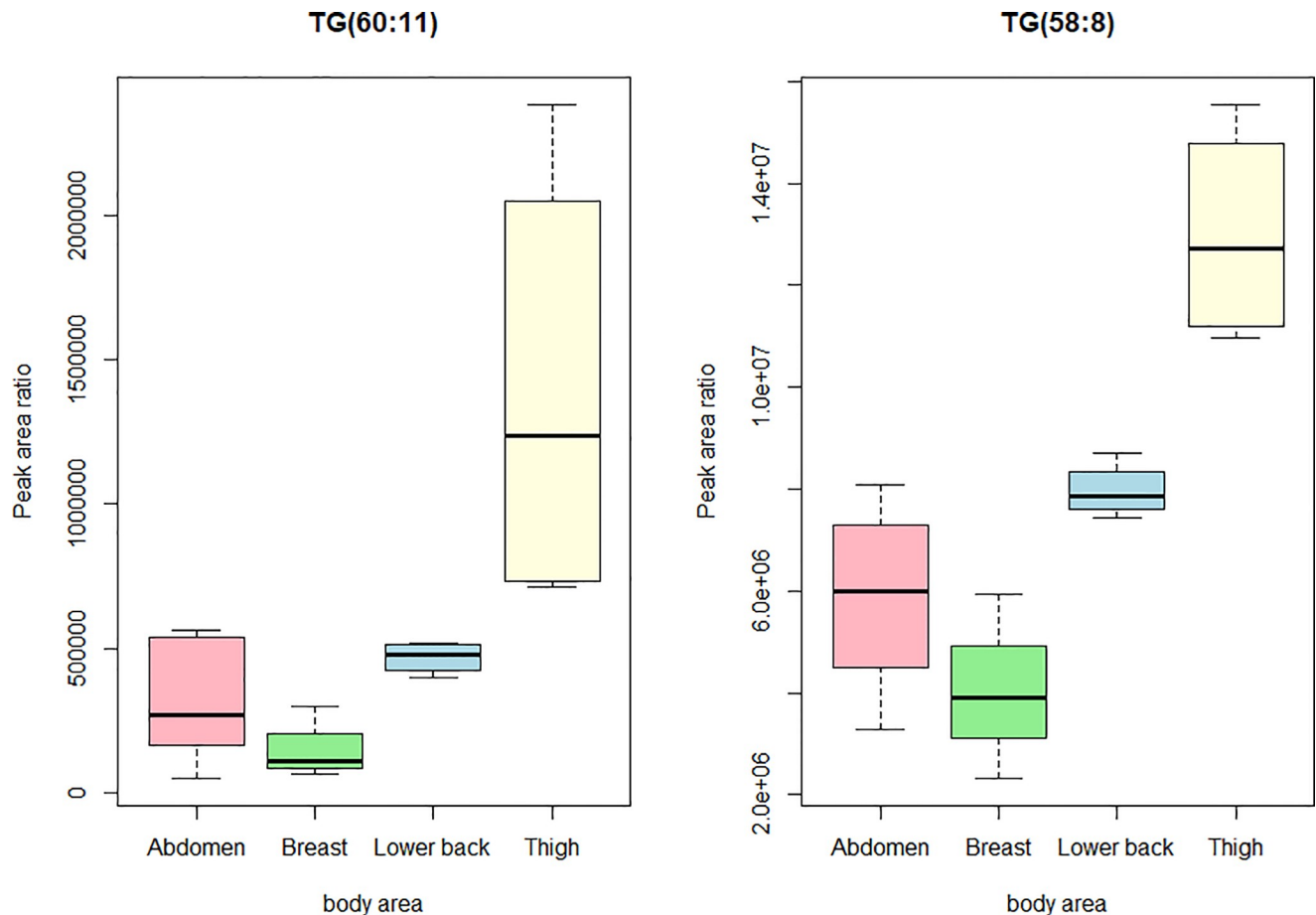


**Fig 5. Boxplots showing the differences between the body areas for two triacylglycerols: The TG(60:11) (left) and the TG(58:8) (right).** Pairwise differences with statistical significance ( $p < 0.01$ ) are highlighted. TG: triacylglycerols.

<https://doi.org/10.1371/journal.pone.0228521.g005>

levels of long polyunsaturated TGs and lower levels of long and medium-sized saturated and low-unsaturated TGs (see the right side of the panel in the “Lower Back vs. Breast” column and the “TG” row in the [S1 Fig](#)).

Finally, no differences between lower back and abdomen or breast and abdomen were statistically significant (see the “Lower Back vs. Abdomen” and “Breast vs. Abdomen” columns in [S1 Fig](#)).

### 3.5 Summary of differences between body areas

In summary, major differences in the lipid composition were observed between thigh and other body areas. The levels of long polyunsaturated TGs were consistently higher in thigh than in other areas and higher levels were also observed in medium-sized polyunsaturated TGs. In contrast, a group of saturated and monounsaturated TGs were lower in thigh than in the other body areas. This observation is noteworthy as Karastergiou *et al.* have shown that individuals with fat accumulated to the thighs show a lower risk for metabolic disease when compared to the accumulation of abdominal fat [50].

The current study was initiated to optimize the methodology for multi-area adipose tissue analysis and to explore, whether different body areas are comparable for adipose tissue

collection. One strength of this study is that we had sufficient human adipose tissue from a single subject to optimize the methodology on homogenous material. Moreover, we tested both the major extraction methods with several body areas to assess potential area-specific variation.

A weakness of the study is its size and the fact that subjects were not a defined cohort; as a methodology development study it was designed with a small number of volunteers. The participants had adipose tissue removed for various reasons but the majority received a cosmetic operation to reduce excess adipose tissue in the central body, thighs or breasts. Hence, the findings of differences in TGs across the body areas should be studied further and their relationship to metabolic disease should be investigated. It would also be desirable to include a sufficient number of participants with simultaneous fat suction one of multiple body areas to enable the within-person comparison between body areas for improved statistical power.

#### 4. Conclusions

This study showed that 2 mg of adipose tissue can produce good quality lipidomics data, acquiring relative levels of almost 200 lipid species belonging to eight lipid classes. The results suggest that adipose tissue in the thigh has a distinct composition of lipids with a higher amount of long polyunsaturated triacylglycerols (TGs), which is different from the lipid composition stored in the body's trunk.

Further, a group of saturated and monounsaturated TGs were in lower levels in thigh compared to breast. This trend was also visible in other comparisons against thigh, although not significant, indicating generally somewhat lower levels of saturated and monounsaturated TGs in thigh. With the limited number of participants, though, it was not possible to investigate this and other patterns of individual variation further with the present study.

We hypothesize that aberrations in the balance of lipid species across the body could hold a key to further understanding the complications of metabolic syndrome. Not only the absolute amount of specific lipids in the body but also their distribution in the adipose tissue across the body might have implications on metabolic outcomes.

As routine clinical assessment of biomarkers from omics technologies becomes increasingly commonplace, we argue that the next frontier of personalized medicine will be to gain a deeper understanding of the balance of biomarkers across the active areas of the body. Depending on the condition, this could be between the blood and tissue, between different organs, or as in this work, between different areas of the same tissue type.

For metabolic disease, the distribution and location-specific content of adipose tissue could explain some missing links to the development of co-morbidities, such as cardiovascular disease, non-alcoholic liver disease and type 2 diabetes. In addition to adipose tissue, also the fat composition of the liver tissue has been shown to play an important role in the development of the metabolic co-morbidities [51]. However, biopsy sampling from the liver is significantly more intrusive an operation than that from the adipose tissue, and thereby it does not carry similar potential for broader adaption in the clinical practice.

On the other hand, increasing numbers of persons with obesity go through liposuction and bariatric operations [52], giving an opportunity also for the routine collection of adipose tissue material for profiling purposes. With the expense and speed of omics profiling technologies becoming increasingly applicable for clinical research and its translation to clinical practice, we expect that the hidden information also from the adipose tissue could be unleashed for the benefit of every patient. The ideas presented here are warranted for further investigation—now possible with the methodology reported in this paper.

## Supporting information

### S1 Method. Detailed description of LC-MS method.

(DOCX)

### S1 Table. Identified lipids from positive ionization mode.

(DOCX)

### S2 Table. Identified lipids from negative ionization mode.

(DOCX)

**S1 Fig. Heatmap of all the comparisons of the lipidome between body areas.** Statistics are grouped by the comparison pair (columns) and the lipid class (rows from DG to TG) into panels. Within each panel, each colored rectangle corresponds to one lipid species, and its location in the x-axis and y-axis, respectively, shows its level of unsaturation (number of double bonds) and its size (number of carbon atoms in the fatty acid chains). Blue, red and white rectangles, respectively, indicate lower, higher and same levels in thigh compared to abdomen (based on the regression coefficient from the linear regression model with the body area as an independent variable and the lipid level as the dependent variable). Statistical significance of the difference is annotated by the symbols “\*,” “x” and “+,” respectively, corresponding to  $p < 0.01$ , 0.05 and 0.1. For instance the comparison between thigh and abdomen is the fourth column from the left. In that comparison, the triacylglycerol TG(60:11) is located in the x- and y-coordinates 11 and 60, respectively, (the top-rightmost corner) in the TG panel. The lipid TG(60:11) has a total of 60 carbon atoms and 11 double bonds (i.e., unsaturated bonds) in its fatty-acid chains. The lipid has a clearly higher level in thigh compared to abdomen (red color of the rectangle) with a statistical significance of  $p < 0.01$  (annotation with the character “\*\*”).

(DOCX)

### S1 File.

(CSV)

## Author Contributions

**Conceptualization:** Ashfaq Ali, Linda Ahonen, Lars Ove Dragsted.

**Data curation:** Naba Al-Sari, Ismo Mattila, Ashfaq Ali, Kajetan Trost, Cristina Legido-Quigley.

**Formal analysis:** Naba Al-Sari.

**Investigation:** Naba Al-Sari.

**Project administration:** Naba Al-Sari, Lars Ove Dragsted, Cristina Legido-Quigley.

**Resources:** Trine Foged Henriksen.

**Software:** Tommi Suvitaival.

**Supervision:** Tommi Suvitaival, Ashfaq Ali, Linda Ahonen, Flemming Pociot, Cristina Legido-Quigley.

**Validation:** Tommi Suvitaival.

**Visualization:** Naba Al-Sari, Tommi Suvitaival.

**Writing – original draft:** Naba Al-Sari, Tommi Suvitaival.

**Writing – review & editing:** Linda Ahonen, Flemming Pociot, Cristina Legido-Quigley.

## References

1. Gadde KM, Martin CK, Berthoud HR, Heymsfield SB. Obesity: Pathophysiology and Management. *J Am Coll Cardiol* 2018; 71:69–84. <https://doi.org/10.1016/j.jacc.2017.11.011> PMID: 29301630
2. Fallahian F, Ardestani A, Pranckevicius E, Raut CP, Tavakkoli A, Sheu EG. The impact of lipomatous tumors on type 2 diabetes: are adipose-derived tumors metabolically active?. *J Surg Res* 2018; 222:48–54. <https://doi.org/10.1016/j.jss.2017.09.040> PMID: 29273375
3. Rahn S, Zimmermann V, Viol F, Knaack H, Stemmer K, Peters L, et al. Diabetes as risk factor for pancreatic cancer: Hyperglycemia promotes epithelial-mesenchymal-transition and stem cell properties in pancreatic ductal epithelial cells. *Cancer Lett* 2018; 415:129–150. <https://doi.org/10.1016/j.canlet.2017.12.004> PMID: 29222037
4. Bergmann K, Sypniewska G. Diabetes as a complication of adipose tissue dysfunction. Is there a role for potential new biomarkers?. *Clin Chem Lab Med* 2013; 51:177–185. <https://doi.org/10.1515/cclm-2012-0490> PMID: 23241684
5. Frasca D, Blomberg BB, Paganelli R. Aging, obesity, and inflammatory age-related diseases. *Front Immunol* 2017; 8:1–10.
6. Succurro E, Segura-Garcia C, Ruffo M, Caroleo M, Rania M, Aloï M, et al. Obese patients with a binge eating disorder have an unfavorable metabolic and inflammatory profile. *Med (United States)* 2015; 94:e2098.
7. Jin B, Liu R, Hao S, Li Z, Zhu C, Zhou X, et al. Defining and characterizing the critical transition state prior to the type 2 diabetes disease. *PLoS One* 2017; 12:e0180937. <https://doi.org/10.1371/journal.pone.0180937> PMID: 28686739
8. Tobin L, Simonsen L, Bülow J. The dynamics of the microcirculation in the subcutaneous adipose tissue is impaired in the postprandial state in type 2 diabetes. *Clin Physiol Funct Imaging* 2011; 31:458–463. <https://doi.org/10.1111/j.1475-097X.2011.01041.x> PMID: 21981457
9. Gealekman O, Guseva N, Hartigan C, Apotheker S, Gorgoglione M, Gurav K, et al. Depot-specific differences and insufficient subcutaneous adipose tissue angiogenesis in human obesity. *CIRC J* 2011; 123:186–194.
10. De Mello VD, Paananen J, Lindström J, Lankinen MA, Shi L., Kuusisto J, et al. Indolepropionic acid and novel lipid metabolites are associated with a lower risk of type 2 diabetes in the Finnish Diabetes Prevention Study. *Sci Rep* 2017; 7:46337. <https://doi.org/10.1038/srep46337> PMID: 28397877
11. Mardinoglu A, Agren R, Kampf C, Asplund A, Nookaew I, Jacobson P, et al. Integration of clinical data with a genome-scale metabolic model of the human adipocyte. *Mol Syst Biol* 2013; 9:649. <https://doi.org/10.1038/msb.2013.5> PMID: 23511207
12. Quehenberger O, Armando AM, Brown AH, Milne SB, Myers DS, Merrill AH, et al. Lipidomics reveals a remarkable diversity of lipids in human plasma. *J Lipid Res* 2010; 51:3299–3305. <https://doi.org/10.1194/jlr.M009449> PMID: 20671299
13. Li-Gao R, de Mutsert R, Rensen PC, van Klinken JB, Prehn C, Adamski J, et al. Postprandial metabolite profiles associated with type 2 diabetes clearly stratify individuals with impaired fasting glucose. *Metabolomics* 2018; 14:13. <https://doi.org/10.1007/s11306-017-1307-7> PMID: 29249917
14. Pandey V, Singh M, Pandey D, Kumar A. Integrated proteomics, genomics, metabolomics approaches reveal oxalic acid as pathogenicity factor in *Tilletia indica* inciting Karnal bunt disease of wheat. *Sci Rep* 2018; 8:7826. <https://doi.org/10.1038/s41598-018-26257-z> PMID: 29777151
15. Sepúlveda-Cisternas I, Lozano Aguirre L, Flores AF, de Ovando IV, García-Angulo VA. Transcriptomics reveals a cross-modulatory effect between riboflavin and iron and outlines responses to riboflavin biosynthesis and uptake in *Vibrio cholerae*. *Sci Rep* 2018; 8:3149. <https://doi.org/10.1038/s41598-018-21302-3> PMID: 29453341
16. Folch-Fortuny A, Bosque G, Picó J, Ferrer A, Elena SF. Fusion of genomic, proteomic and phenotypic data: The case of potyviruses. *Mol Biosyst* 2016; 12:253–261. <https://doi.org/10.1039/c5mb00507h> PMID: 26593691
17. Qiu G, Zheng Y, Wang H, Sun J, Ma H, Xiao Y, et al. Plasma metabolomics identified novel metabolites associated with risk of type 2 diabetes in two prospective cohorts of Chinese adults. *Int J Epidemiol* 2016; 45:1507–1516. <https://doi.org/10.1093/ije/dyw221> PMID: 27694567
18. Pritchard JM, Karampatos S, Beattie KA, Giangregorio LM, Ioannidis G, Atkinson SA, et al. The Relationship between Intramuscular Adipose Tissue, Functional Mobility, and Strength in Postmenopausal Women with and without Type 2 Diabetes. *J Aging Res* 2015; 2015:1–9.
19. Lee H-C, Yokomizo T. Applications of mass spectrometry-based targeted and non-targeted lipidomics. *Biochem Biophys Res Commun* 2018; 504:576–581. <https://doi.org/10.1016/j.bbrc.2018.03.081> PMID: 29534960

20. Christinat N, Masoodi M. Comprehensive Lipoprotein Characterization Using Lipidomics Analysis of Human Plasma. *J Proteome Res* 2017; 16:2947–2953. <https://doi.org/10.1021/acs.jproteome.7b00236> PMID: 28650171
21. Huang X, Sjögren P, Cederholm T, Ärnlov J, Lindholm B, Risérus U, et al. Serum and adipose tissue fatty acid composition as biomarkers of habitual dietary fat intake in elderly men with chronic kidney disease. *Nephrol Dial Transplant* 2014; 29:128–136. <https://doi.org/10.1093/ndt/gfs478> PMID: 23229929
22. Baylin A, Campos H. The use of fatty acid biomarkers to reflect dietary intake. *Curr Opin Lipidol* 2006; 17:22–27. <https://doi.org/10.1097/01.mol.0000199814.46720.83> PMID: 16407712
23. Wolk A, Furuheim M, Vessby B. Fatty acid composition of adipose tissue and serum lipids are valid biological markers of dairy fat intake in men. *J Nutr* 2001; 131:828–833. <https://doi.org/10.1093/jn/131.3.828> PMID: 11238766
24. Matyash V, Liebisch G, Kurzchalia TV, Shevchenko A, Schwudke D. Lipid extraction by methyl-tert-butyl ether for high-throughput lipidomics. *J Lipid Res* 2008; 49:1137–1146. <https://doi.org/10.1194/jlr.D700041-JLR200> PMID: 18281723
25. Al-Sulaiti H, Diboun I, Banu S, Al-Emadi M, Amani P, Harvey T, et al. Triglyceride profiling in adipose tissues from obese insulin sensitive, insulin resistant and type 2 diabetes mellitus individuals. *J Transl Med* 2018; 16:1–13.
26. Moreno-Navarrete JM, Linãres-Pose L, Sabater M, Rial-Pensado E, Comas F, Jové M, et al. Adipose TSHB in humans and serum TSH in hypothyroid rats inform about cellular senescence. *Cell Physiol Biochem* 2018; 51:142–153. <https://doi.org/10.1159/000495170> PMID: 30448824
27. Tomášová P, Čermáková M, Pelantová H, Vecka M, Kratochvílová H, Lipš M, et al. Minor lipids profiling in subcutaneous and epicardial fat tissue using LC/MS with an optimized preanalytical phase. *J Chromatogr B Anal Technol Biomed Life Sci* 2019; 1113:50–59.
28. Liesenfeld DB, Grapov D, Fahrman JF, Schneider Salou Schneider M, Scherer D, Toth R, et al. Metabolomics and transcriptomics identify pathway differences between visceral and subcutaneous adipose tissue in colorectal cancer patients: The ColoCare study. *Am J Clin Nutr* 2015; 102:433–443. <https://doi.org/10.3945/ajcn.114.103804> PMID: 26156741
29. Baker RC, Nikitina Y, Subauste AR. Chapter Six—Analysis of adipose tissue lipid using mass spectrometry. In: *Meth Enzymol* 2014; 538:89–105. <https://doi.org/10.1016/B978-0-12-800280-3.00006-2> PMID: 24529435
30. Roberts LD, West JA, Vidal-Puig A, Griffin JL. Methods for performing lipidomics in white adipose tissue. In: *Meth Enzymol* 2014; 538:211–231. <https://doi.org/10.1016/B978-0-12-800280-3.00012-8> PMID: 24529441
31. López-Bascón MA, Calderón-Santiago M, Sánchez-Ceinos J, Fernández-Vega A, Guzmán-Ruiz R, López-Miranda J, et al. Influence of sample preparation on lipidomics analysis of polar lipids in adipose tissue. *Talanta* 2018; 177:86–93. <https://doi.org/10.1016/j.talanta.2017.09.017> PMID: 29108587
32. Sedger LM, Tull DL, McCornville MJ, De Souza DP, Rupasinghe TW, Williams SJ, et al. Lipidomic profiling of adipose tissue reveals an inflammatory signature in cancer-related and primary Lymphedema. *PLoS One* 2016; 11:e0154650. <https://doi.org/10.1371/journal.pone.0154650> PMID: 27182733
33. Folch J, Lees M, Sloane Stanley GH. A simple method for the isolation and purification of total lipids from animal tissues. *J Biol Chem* 1957; 226:497–509. PMID: 13428781
34. O’Gorman A, Suvitaival T, Ahonen L, Cannon M, Zammit S, Lewis G, et al. Identification of a plasma signature of psychotic disorder in children and adolescents from the Avon Longitudinal Study of Parents and Children (ALSPAC) cohort. *Transl Psychiatry* 2017; 7:e1240. <https://doi.org/10.1038/tp.2017.211> PMID: 28949339
35. Luukkonen PK, Zhou Y, Nidhina Haridas PA, Dwivedi OP, Hyötyläinen T, Ali A, et al. Impaired hepatic lipid synthesis from polyunsaturated fatty acids in TM6SF2 E167K variant carriers with NAFLD. *J Hepatol* 2017; 67:128–136. <https://doi.org/10.1016/j.jhep.2017.02.014> PMID: 28235613
36. Lamichane S, Ahonen L, Dyrlund TS, Kempainen E, Siljander H, Hyöty H, et al. Dynamics of Plasma Lipidome in Progression to Islet Autoimmunity and Type 1 Diabetes-Type 1 Diabetes Prediction and Prevention Study (DIPP). *Sci Rep* 2018; 8:10635. <https://doi.org/10.1038/s41598-018-28907-8> PMID: 30006587
37. Lamichane S, Ahonen L, Dyrlund TS, Siljander H, Hyöty H, Ilonen J, et al. A longitudinal plasma lipidomics dataset from children who developed islet autoimmunity and type 1 diabetes. *Sci Data* 2018; 5:180250. <https://doi.org/10.1038/sdata.2018.250> PMID: 30422126
38. Mzmine A. MZmine 2.6 manual. *BMC Bioinformatics*. 2012;(c):2005–2012.
39. Fahy E, Sud M, Cotter D, Subramaniam S. LIPID MAPS online tools for lipid research. *Nucleic Acids Res* 2007; 35:W606–W612. <https://doi.org/10.1093/nar/gkm324> PMID: 17584797

40. Bowden JA, Heckert A, Ulmer CZ, Jones CM, Koelmel JP, Abdullah L, et al. Harmonizing Lipidomics: NIST Interlaboratory Comparison Exercise for Lipidomics using Standard Reference Material 1950 Metabolites in Frozen Human Plasma. *J Lipid Res* 2017; 58:jlrm079012.
41. Sumner LW, Reily MD, Higashi R, Nicholls AW, Marriott P, Hardy N, et al. Proposed minimum reporting standards for chemical analysis. *Metabolomics* 2007; 3:211–221. <https://doi.org/10.1007/s11306-007-0082-2> PMID: 24039616
42. The R Project for Statistical Computing. <https://www.r-project.org/>. Accessed: 1 Aug 2019.
43. Lê S, Josse J FH. FactoMineR: An R Package for Multivariate Analysis. *J Stat Softw* 2008; 25:1–18.
44. Ritchie ME, Phipson B, Wu D, Hu Y, Law CW, Shi W, et al. limma powers differential expression analyses for RNA-sequencing and microarray studies. *Nucleic Acids Res* 2015; 43:e47. <https://doi.org/10.1093/nar/gkv007> PMID: 25605792
45. Wickham H. ggplot2: Elegant Graphics for Data Analysis. Springer-Verlag New York 2016.
46. Slomiany A, Slomiany BL. A new method for the isolation of the simple and highly complex glycosphingolipids from animal tissue. *J Biochem Biophys Methods* 1981; 5:229–236. [https://doi.org/10.1016/0165-022x\(81\)90047-6](https://doi.org/10.1016/0165-022x(81)90047-6) PMID: 7310045
47. Whiley L, Godzien J, Ruperez F J, Legido-Quigley C, Barbas C. In-Vial Dual Extraction for Direct LC-MS Analysis of Plasma for Comprehensive and Highly Reproducible Metabolic Fingerprinting. *Anal Chem* 2012; 84:5992–5999. <https://doi.org/10.1021/ac300716u> PMID: 22702345
48. Snowden SG, Ebshiana AA, Hye A, An Yang, Pletnikova O, O'Brien R, et al. Association between fatty acid metabolism in the brain and Alzheimer disease neuropathology and cognitive performance: A non-targeted metabolomic study. *PLoS Med* 2017; 14:1–19.
49. Zhang H, Gao Y, Sun J, Fan S, Yao X, Ran X, et al. Optimization of lipid extraction and analytical protocols for UHPLC-ESI-HRMS-based lipidomic analysis of adherent mammalian cancer cells. *Anal Bioanal Chem* 2017; 409:5349–5358. <https://doi.org/10.1007/s00216-017-0483-7> PMID: 28717896
50. Karastergiou K, Fried SK, Xie H, Lee MJ, Divoux A, Rosencrantz MA, et al. Distinct developmental signatures of human abdominal and gluteal subcutaneous adipose tissue depots. *J Clin Endocrinol Metab* 2013; 98:362–371. <https://doi.org/10.1210/jc.2012-2953> PMID: 23150689
51. Ščupáková K, Soons Z, Ertaylan G, Pierzchalski KA, Eijkel GB, Ellis SR, et al. Spatial systems lipidomics reveal nonalcoholic fatty liver disease heterogeneity. *Anal Chem* 2018; 90:5130–5138. <https://doi.org/10.1021/acs.analchem.7b05215> PMID: 29570976
52. Picot J, Jones J, Colquitt JL, Gospodarevskaya E, Loveman E, Baxter L, et al. The clinical effectiveness and cost-effectiveness of bariatric (weight loss) surgery for obesity: a systematic review and economic evaluation. *Health Technol Assess* 2009; 13:1–190.